



Research article

Asn336 is involved in the substrate affinity of glycine oxidase from *Bacillus cereus*



Gaobing Wu^a, Tao Zhan^b, Yiming Guo^b, Ashok Kumar^b, Ziduo Liu^{b,*}

^a State Key Laboratory of Agricultural Microbiology, College of Plant Science and Technology, Huazhong Agricultural University, Wuhan 430070, China

^b State Key Laboratory of Agricultural Microbiology, College of Life Science and Technology, Huazhong Agricultural University, Wuhan 430070, China

ARTICLE INFO

Article history:

Received 5 October 2015

Accepted 13 May 2016

Available online 05 June 2016

Keywords:

Bacillus cereus

Error-prone PCR

Glycine oxidase

Site-directed mutagenesis

Substrate affinity

ABSTRACT

Background: Glycine oxidase (GO), a type of D-amino acid oxidase, is of biotechnological interest for its potential in several fields. In our previous study, we have characterized a new glycine oxidase (BceGO) from *Bacillus cereus* HYC-7. Here, a variant of N336K with increased the affinity against all the tested substrate was obtained by screening a random mutant library of BceGO. It is observed that the residue N336 is invariable between its homogeneous enzymes. This work was aimed to explore the role of the residue N336 in glycine oxidase by site-directed mutagenesis, kinetic assay, structure modeling and substrate docking.

Results: The results showed that the affinity of N336H, N336K and N336R increased gradually toward all the substrates, with increase in positive charge on side chain, while N336A and N336G have not shown a little significant effect on substrate affinity. The structure modeling studies indicated that the residue Asn336 is located in a random coil between β -18 and α -10. Also, far-UV CD spectra-analysis showed that the mutations at Asn336 do not affect the secondary structure of enzyme.

Conclusion: Asn336 site was located in a conserved GHYRNG loop which adjoining to substrate and the isoalloxazine ring of FAD, and involved in the substrate affinity of glycine oxidase. This might provide new insight into the structure–function relationship of GO, and valuable clue to redesign its substrate specificity for some biotechnological application.

© 2016 Pontificia Universidad Católica de Valparaíso. Production and hosting by Elsevier B.V. All rights reserved.

1. Introduction

Glycine oxidase (GO, EC 1.4.3.19), a homotetrameric flavoenzyme, contains non-covalently attached FAD molecule [1,2]. BceGO catalyzes the oxidative deamination of various amines (glycine, sarcosine, N-ethylglycine) and some D-isomer of amino acids (D-alanine, D-proline, etc.) to yield corresponding α -keto acid(s), ammonia/amine, and hydrogen peroxide. GO appears to be stereo-specific in oxidizing the D-amino acids and its substrate specificity partially similar to D-amino acid oxidase (DAAO, EC 1.4.3.3) and sarcosine oxidase (SOX, EC 1.5.3.1). It plays an important role in the biosynthesis of the thiazole ring of thiamine pyrophosphate cofactors in *Bacillus subtilis* [2]. The broad substrate specificity and stereoselectivity of GO confers it great potential in several biotechnological fields, such as industrial biocatalysis, biosensors and developing glyphosate-resistant crop [3,4,5]. This promotes scientists to search new enzyme, study the structure–function relationship and redesign its application by protein engineering [5,6].

In our previous study, we have reported a new glycine oxidase (BceGO) with glyphosate-oxidative activity from *Bacillus cereus* and, developed a high through screening method for improving its affinity and activity toward glyphosate [7]. Here, we continued to screen new mutant with higher specificity to glyphosate from a random mutation library of BceGO, and obtained a mutant, N336K, whose $K_{m, app}$ on glyphosate decreased 3.77-fold. Sequence alignment showed that the residue N336 is highly conserved in BceGO and its homogeneous enzymes. Here, we attempted to investigate the role of N336 residue in the catalytic activity of GO by site-directed mutagenesis, three-dimensional structure modeling and ligand docking assay.

2. Materials and methods

2.1. Reagents, strains, and plasmid

Glyphosate, glycine, sarcosine, D-alanine, o-dianisidine dihydrochloride, horseradish peroxidase and FAD were purchased from Sigma (USA). Taq DNA polymerase, T4 DNA ligase and restriction enzymes were purchased from TAKARA (Japan). Fast Pfu polymerase, DNA purification kits, GST Binding Resin and Bradford protein assay kits were acquired from TransGen (Beijing, China), Axygen (USA), Novagen (Germany), and

* Corresponding author.

E-mail address: lzd@mail.hzau.edu.cn (Z. Liu).

Peer review under responsibility of Pontificia Universidad Católica de Valparaíso.

Table 1

Primers used for gene BceGO mutagenesis. The BamHI and XhoI sites were italic and underlined, and the mutation positions were underlined.

Target sites	Sequence (5'-3')
BceGO-F	CGCGGATCCATGTGTAGAAGTATGATGTAGCGAT
BceGO-R	CCGCTCGAGCTAAACBTTYTAGAAAGCAATGAAT
N336H-F	GGCCATTATCGACATGGTATTTTAT
N336H-R	ATGTCGATAATGGCCCGTGCAAGTA
N336R-F	GGCCATTATCGACGTGGTATTTTAT
N336R-R	ACGTCGATAATGGCCCGTGCAAGTA
N336A-F	GGCCATTATCGAGCGGGTATTTTAT
N336A-R	CGCTCGATAATGGCCCGTGCAAGTA
N336G-F	GGCCATTATCGAGCGGTATTTTAT
N336G-R	GCCTCGATAATGGCCCGTGCAAGTA

Sangon (Shanghai, China), respectively. *Escherichia coli* DH5 α and *E. coli* BL21 (DE3) were used as for gene cloning and for protein expression, respectively.

2.2. Construction of mutant library and site-directed mutagenesis

The BceGO random mutant library was generated by error-prone PCR used pGEX-GO as the template. The amplification mixture, which contained 20 nM primers, 0.2 mM dATP and dCTP, 0.1 mM dTTP and dGTP, 2 U Taq DNA polymerase and Taq buffer containing 5 mM MgCl₂ and 0.5 mM MnCl₂ in 100 μ L volume, was cycled in an Bio-rad thermal cycler (California, USA) for 30 cycles of 94°C for 30 s, 57°C for 30 s, and 72°C for 70 s. PCR products were purified, digested with BamHI and XhoI, cloned into pGEX-6P-1, and transformed into *E. coli* DH5 α to obtain the random mutant library.

PCR-based site-directed mutagenesis was carried out to generate single-mutant [8]. PCR reactions (50 μ L) contained 20 ng template (pGEX-GO), 0.2 mM dNTP, 20 nM each primer, 10 μ L PCR buffer and 1 unit of *Pfu* DNA polymerase (Transgen, China). The PCR cycling parameters were: 1 cycle of 2 min at 97°C, 20 cycles of 20 s at 95°C, 30 s at 54°C, and 160 s at 72°C, and incubation of 10 min at 72°C. Then the PCR products were treated with *DpnI* to digest the parental DNA at 37°C for 8 h. Finally, *DpnI* digestion mixture was transformed into *E. coli* DH5 α competent cells, and the transformant was selected on ampicillin plates. The primers used were listed in Table 1. The desired mutants were validated by DNA sequencing.

2.3. Screening for GO mutants

The mutant library was screened by an enzyme-coupled assay using horseradish peroxidase (5 U/mL) and *o*-dianisidine dihydrochloride as described previously [9]. Single colony from random mutation library was cultured in deep-well plates containing 0.6 mL LB medium, and induced by IPTG. Then cell extracts containing target protein were prepared by adding the bacteriophage T7. To screen mutants with higher specificity to glyphosate, 100 μ L of each cell lysate was

incubated with 20 μ L of 50 mM glyphosate, 20 μ L of 0.32 mg/mL *o*-dianisidine dihydrochloride, and 1 μ L of 5 U/mL horseradish peroxidase in sodium phosphate buffer (50 mM; pH 8.5) followed by measuring the absorbance values at 450 nm. Mutants showed higher absorbance than the wild-type were selected for further activity analysis.

2.4. Enzyme expression and purification

The recombinant BceGO and its mutant were purified by affinity chromatography using the methods described previously [7]. Briefly, the recombinant plasmids were transformed into the host *E. coli* BL21 (DE3). Recombinant cells grew at 37°C in LB medium containing 100 μ g/mL ampicillin. Protein expression was induced by adding isopropyl β -D-1-thiogalactopyranoside (IPTG) at a final concentration of 0.2 mM, when the OD₆₀₀ reached 0.6. After an overnight induction at 22°C, 1.5 L culture was collected and disrupted by the high pressure homogenizer (NiroSoavi, Italy). Then, the supernatant of the lysate was mixed with 1.5 mL GST-Bind Resin that had been equilibrated with 50 mM disodium pyrophosphate buffer. The resin was washed with disodium pyrophosphate buffer (50 mM, pH 7.5) to elute the unspecific-binding protein. Finally, the GST-free recombinant protein was prepared by on-column cleavage with PreScission protease [10]. The concentration of the wild-type BceGO and mutants was measured by the method of Bradford assay [11]. The purity of the protein was analyzed by sodium dodecyl sulfate polyacrylamide gel electrophoresis (SDS-PAGE).

2.5. Determination of kinetic parameters

The kinetic parameters of wild-type BceGO and mutants were assayed using a fixed amount of enzyme and various concentration of substrates (glycine, 0–300 mM; glyphosate, 0–600 mM; sarcosine, 0–300 mM; D-alanine, 0–600 mM). The absorbance was measured at 450 nm using a microplate reader (Thermo Scientific, Multiscan spectrum). The initial reaction velocities under various concentrations of each substrate were fitted to the Lineweaver-Burk transformation of the Michaelis–Menten equation to figure out apparent kinetic parameters (i.e., $K_{m,app}$ and V_{max}). Further, the $k_{cat,app}$ was calculated by the equation: $k_{cat,app} = V_{max} / [E]$, in which $[E]$ is the total amount of enzyme in the reaction mixture.

2.6. Circular dichroism and secondary structure prediction

Secondary structure of BceGO was predicted by using the program PSIPRED [12]. Circular dichroism (CD) spectra of BceGO and variants were recorded with a Jasco-810 CD spectrometer (Jasco Corp., Japan). The data were collected at room temperature from 190 to 260 nm using 1 mm quartz cuvette (400 μ L). The conversion to the Mol CD ($\Delta\epsilon$) in each spectrum was performed with the Jasco Standard Analysis software. Estimation of the secondary structure content from far-UV circular dichroism (CD) spectra was performed by using the CDPPro

Table 2

Comparison of the apparent kinetics parameters of the wild-type BceGO and the mutants toward different substrates.

		Wild-type	N336H	N336K	N336R	N336A	N336G
Glycine	$k_{cat,app}$ (s^{-1})	0.71 \pm 0.03	0.37 \pm 0.02	0.25 \pm 0.003	0.024 \pm 0.0002	0.52 \pm 0.02	0.67 \pm 0.03
	$K_{m,app}$ (mM)	1.04 \pm 0.12	0.95 \pm 0.11	0.79 \pm 0.12	0.53 \pm 0.07	1.41 \pm 1.23	2.25 \pm 2.52
	k_{cat}/K_m	0.68	0.39	0.32	0.045	0.37	0.3
Glyphosate	$k_{cat,app}$ (s^{-1})	0.87 \pm 0.02	0.23 \pm 0.05	0.19 \pm 0.002	0.021 \pm 0.0003	0.67 \pm 0.08	0.62 \pm 0.02
	$K_{m,app}$ (mM)	84.79 \pm 2.34	42.31 \pm 1.84	22.45 \pm 1.44	10.44 \pm 0.33	68.36 \pm 3.15	96.73 \pm 2.81
	k_{cat}/K_m	0.01	0.0054	0.0084	0.002	0.0098	0.0064
Sarcosine	$k_{cat,app}$ (s^{-1})	0.98 \pm 0.01	0.68 \pm 0.04	0.28 \pm 0.003	0.035 \pm 0.0002	0.26 \pm 0.03	0.59 \pm 0.04
	$K_{m,app}$ (mM)	1.51 \pm 0.18	1.39 \pm 0.15	0.36 \pm 0.02	0.15 \pm 0.006	1.56 \pm 0.17	2.72 \pm 1.35
	k_{cat}/K_m	0.65	0.49	0.78	0.23	0.17	0.22
D-Alanine	$k_{cat,app}$ (s^{-1})	0.81 \pm 0.04	0.37 \pm 0.03	0.21 \pm 0.001	0.028 \pm 0.0004	0.65 \pm 0.01	0.46 \pm 0.15
	$K_{m,app}$ (mM)	34.65 \pm 1.22	24.63 \pm 1.12	6.81 \pm 0.32	1.31 \pm 0.04	37.6 \pm 0.95	48.85 \pm 1.86
	k_{cat}/K_m	0.023	0.015	0.03	0.021	0.017	0.009



Fig. 1. Protein sequence alignment assay. The sequence alignment was according to sites Gly258 and Glu357 of BceGO. The conserved residues were shaded in black by using the BioEdit program, and the site N336 was marked out by a black triangle. The β -strands and α -helices in this region were indicated with an arrow according to the crystal structure of *B. subtilis* GO [17]. GO used for alignment was derived from *B. subtilis* (Protein Data Bank code: 1RYI), *B. cereus* (GenBank accession NO. KC203486), *B. thuringiensis* (GenBank accession NO. YP034985.1), *B. anthracis* (GenBank accession NO. NP843255.1), *B. amyloliquefaciens* (GenBank accession NO. YP005129858.1), *B. pumilus* (GenBank accession NO. ZP03053300.1), *P. fluorescens* (GenBank accession NO. YP262378.1), *P. mendocina* (GenBank accession NO. YP001186464.1), *Acinetobacter* sp. RUH2624 (GenBank accession NO. ZP05825844.1) and *Paenibacillus* sp. JDR-2 (GenBank accession NO. YP003014095.1), respectively.

software package (available at <http://lamar.colostate.edu/~sreeram/CDPro/main.html>), including three executable programs (SELCON3, CDSSTR, and CONTIN/LL) [13]. In this study, the percentages of α -helix and β -sheet for each protein sample were averaged by the calculations of results from the CDPro software package. The circular dichroism data were expressed in terms of the mean residue ellipticity (θ_{mrw}), which were calculated using Equation 1 [14]:

$$\theta_{mrw} = \frac{M_w \cdot \theta_{obs} \cdot 100}{N \cdot d \cdot c} \quad [\text{Equation 1}]$$

where θ_{obs} is the observed ellipticity in degrees, M_w is the molecular weight of wild-type and variants proteins, and N is the number of residues in BceGO (369), d is the path length of quartz cuvette (0.1 cm), c is the protein concentration (mg/mL), and the constant number 100 stems from the conversion of the molecular weight to mg/dmol.

2.7. Molecular modeling analysis

To obtain a reasonable model, the structure of BceGO was built with homology modeling in InsightII program (version 2005). The crystal structure of glycine oxidase from *B. subtilis* (Protein Data Bank code: 1RYI) was used as the template. The binding conformation of the ligands in the BceGO active site was obtained with the docking module in MOE 2009.10, and the result description was prepared using software PyMol 0.99.

3. Results and discussion

3.1. Mutagenesis of BceGO

A random mutant library of BceGO was constructed by error-prone PCR to screen new mutants with low affinity and increased activity

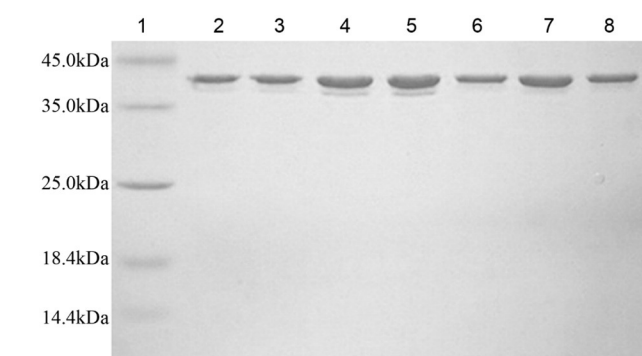


Fig. 2. SDS-PAGE of the purified wild-type BceGO and the mutants. Lane 1, the standard protein markers; lane 2, the wild-type; lanes 3–8: N336H, N336K, N336R, N336A, N336G.

toward glyphosate by the method of high throughput colorimetric assay. Asn336Lys mutant was selected from 7000 clones, which showed improved specificity toward glyphosate than the wild type. Its apparent K_m value decreased 3.77, 1.32, 4.19 and 5.09-fold glyphosate, glycine, sarcosine and D-alanine, respectively (Table 2). However, the turnover numbers (the $k_{cat,app}$) were lower than the wild-type BceGO. Protein sequence alignment showed that Asn336 is highly conserved in the GO family, and locates in the loop connecting β -strands 18 and α -helices 10 (Fig. 1). To elucidate the role of this invariable Asn336, it was substituted with other positively charged amino acids (i.e., His and Arg) and small amino acids (i.e., Ala and Gly) by site-directed mutagenesis.

3.2. Purification of BceGO and its variants

In order to characterize the enzyme, the wild-type BceGO and variants with GST tag were produced in *E. coli* BL21 (DE3) and purified by GSH-agarose affinity chromatography. GST-free recombinant fusion proteins were prepared via on-column cleavage by using PreScission protease. As a result, target proteins with high homogeneity and apparent molecular masses of 41 kDa were obtained (Fig. 2).

3.3. Kinetic parameters of BceGO variants

As shown in Table 2, it was observed that $K_{m,app}$ values against all substrates (i.e., glycine, glyphosate, sarcosine and D-Alanine) declined alone with the increase of positive charge on the side chain of residue 336. Especially, the k_{cat} values of N336R toward substrates decreased 28–41-fold as compared to wild-type BceGO. It means that substitution at N336 with positively charged residues is able to improve the affinity

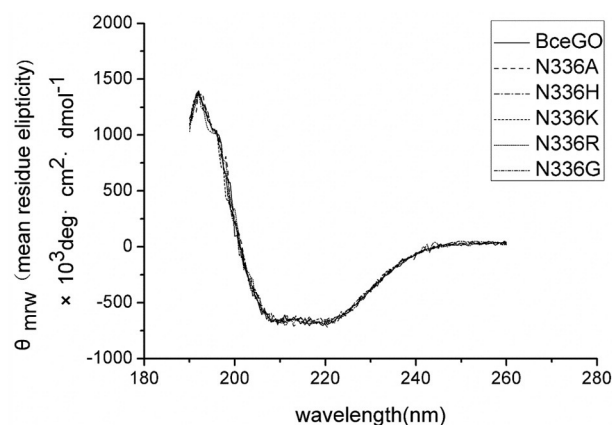


Fig. 3. Circular dichroism spectrum of wild-type BceGO and mutants (N336A, N336H, N336K, N336R, N336G) in 10 mM disodium pyrophosphate buffer (pH 7.5) at 25°C.

Table 3

Secondary structure of GO and variants were calculated by SELCON3 program (CDPro software package).

Components (%)	Wild-type	N336A	N336H	N336K	N336R	N336G
α-Helix	20	20	21	20	19	19
β-Sheet	29	29	30	28	29	29
Turn	20	21	19	22	22	19
Random	31	30	30	30	30	33

for the substrates. The both substitutions N336A and N336G did not significantly affect the substrate affinity (the $K_{m,app}$ value) for all the substrates. Additionally, the turnover number (k_{cat}) of the five mutants toward all tested substrate decreased to some different degrees (Table 2), suggesting that Asn336 is also involved in the catalytic efficiency of BceGO.

3.4. Analysis of protein secondary structure

The program PSIPRED predicted that the residue Asn336 was located in a conservative random coil region. A quantitative analysis of the protein secondary structure for wild-type BceGO and variants has been carried out using SELCON3 program. The data showed that the CD spectra of wild-type GO and mutants (N336H, N336K, N336R, N336A and N336G) were similar (Fig. 3, Table 3). This result suggested that the mutation at Asn336 did not affect the content in secondary structure.

3.5. Structure modeling and substrate docking analysis

Protein homology modeling and ligand docking assay revealed the substrates matching the BceGO active site and orientated to the isoalloxazine ring of the flavin cofactor (Fig. 4). The three dimensional structure of GO from *B. subtilis* showed the active site of GO containing FAD-binding domain and substrate-binding domain including a conserved Rossmann fold $\beta\alpha\beta$ motif. Both theoretical and experimental studies have indicated that the positive charge in the vicinity of the active site could promote the redox potential of the flavin [15]. The carboxylic groups of the substrates through a double bridge to the Arg308 side chain, and the other side of substrates directing toward the active site entrance, might interact with Gly51, Ala54 backbones, and

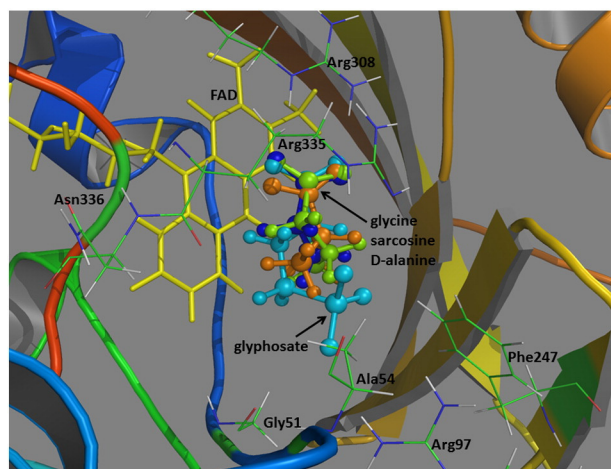


Fig. 4. Protein homology modeling and ligand docking assay. The structure of BceGO was generated by homology modeling in InsightII 2005 with GO from *B. subtilis* (PDB code: 1RY1) as the template. Ligand docking assay was carried out with the docking module in MOE 2009.10. The cofactor FAD was colored in yellow, and the substrates were rendered as ball-and-stick representations (Cyan, glyphosate. Blue, glycine. Green, sarcosine. Tan, D-alanine). This figure was prepared with Pymol 0.99.

side chains of Arg335 and Asn336. The random coil containing Asn336 formed a bulge at the bottom of active cavity, and the mutation at this site might cause alteration in the loop connecting β -strands 18 and α -helices 10, thereby impacting the charge distribution in vicinity of the flavin. In this work, introduction of basic amino acid to site 336 didn't impair BceGO secondary structure and increased the affinity (the $K_{m,app}$ value) to all substrates, indicating that the positive charge near the flavin contributed to the binding of substrates to BceGO, which was accordant with previous findings [16].

4. Conclusion

In this work, we investigated the role of Asn336 in the active cavity of BceGO. Together with experimental data and model analysis, it was concluded that the high conserved residue Asn336 played a crucial role in the substrate affinity of BceGO, and positively charged residue could improve its substrate affinity, significantly. This study provides new insights into the structure–function relationship of glycine oxidase and valuable clue to redesign the substrate specificity by protein engineering.

Financial support

This work was supported by Specialized Research Fund for the Doctoral Program of Higher Education (No. 20120146120014) and the Genetically Modified Organisms Breeding Major Projects of China (2011zx08001-001).

Conflict of interest statement

There are no conflicts of interest.

References

- [1] Job V, Marcone GL, Piloni MS, Pollegioni L. Glycine oxidase from *Bacillus subtilis*. Characterization of a new flavoprotein. *J Biol Chem* 2002;277:6985–93. <http://dx.doi.org/10.1074/jbc.M111095200>.
- [2] Settembre EC, Dorrestein PC, Park JH, Augustine AM, Begley TP, Ealick SE. Structural and mechanistic studies on ThiO, a glycine oxidase essential for thiamin biosynthesis in *Bacillus subtilis*. *Biochemistry* 2003;42:2971–81. <http://dx.doi.org/10.1021/bi026916v>.
- [3] Nicolai A, Ferradini N, Molla G, Biagetti E, Pollegioni L, Veronesi F, et al. Expression of an evolved engineered variant of a bacterial glycine oxidase leads to glyphosate resistance in alfalfa. *J Biotechnol* 2014;184:201–8. <http://dx.doi.org/10.1016/j.biotech.2014.05.020>.
- [4] Rosini E, Piubelli L, Molla G, Frattini L, Valentino M, Varriale A, et al. Novel biosensors based on optimized glycine oxidase. *FEBS J* 2014;281:3460–72. <http://dx.doi.org/10.1111/febs.12873>.
- [5] Pollegioni L, Molla G. New biotech applications from evolved D-amino acid oxidases. *Trends Biotechnol* 2011;29:276–83. <http://dx.doi.org/10.1016/j.tibtech.2011.01.010>.
- [6] Martinez-Martinez I, Navarro-Fernandez J, Garcia-Carmona F, Takami H, Sanchez-Ferrer A. Characterization and structural modeling of a novel thermostable glycine oxidase from *Geobacillus kaustophilus* HTA426. *Proteins Struct Funct Bioinf* 2008;70:1429–41. <http://dx.doi.org/10.1002/prot.21690>.
- [7] Zhan T, Zhang K, Chen YY, Lin YJ, Wu GB, Zhang LL, et al. Improving glyphosate oxidation activity of glycine oxidase from *Bacillus cereus* by directed evolution. *PLoS One* 2013;8, e79175. <http://dx.doi.org/10.1371/journal.pone.0079175>.
- [8] Weiner MP, Costa GL, Schoettlin W, Cline J, Mathur E, Bauer JC. Site-directed mutagenesis of double-stranded DNA by the polymerase chain reaction. *Gene* 1994;151:119–23. [http://dx.doi.org/10.1016/0378-1119\(94\)90641-6](http://dx.doi.org/10.1016/0378-1119(94)90641-6).
- [9] Tarahovsky YS, Ivanitsky GR, Khushainov AA. Lysis of *Escherichia coli* cells induced by bacteriophage T4. *FEMS Microbiol Lett* 1994;122:195–9. <http://dx.doi.org/10.1111/j.1574-6968.1994.tb07164.x>.
- [10] Dian C, Eshaghi S, Urbig T, McSweeney S, Heijbel A, Salbert G, et al. Strategies for the purification and on-column cleavage of glutathione-S-transferase fusion target proteins. *J Chromatogr B* 2002;769:133–44. [http://dx.doi.org/10.1016/S1570-0232\(01\)00637-7](http://dx.doi.org/10.1016/S1570-0232(01)00637-7).
- [11] Bradford MM. A rapid and sensitive method for the quantitation of microgram quantities of protein utilizing the principle of protein-dye binding. *Anal Biochem* 1976;72:248–54. [http://dx.doi.org/10.1016/0003-2697\(76\)90527-3](http://dx.doi.org/10.1016/0003-2697(76)90527-3).
- [12] McGuffin LJ, Bryson K, Jones DT. The PSIPRED protein structure prediction server. *Bioinformatics* 2000;16:404–5. <http://dx.doi.org/10.1093/bioinformatics/16.4.404>.
- [13] Sreerama N, Woody RW. Estimation of protein secondary structure from circular dichroism spectra: Comparison of CONTIN, SELCON, and CDSSTR methods with an expanded reference set. *Anal Biochem* 2000;287:252–60. <http://dx.doi.org/10.1006/abio.2000.4880>.

- [14] Chaloupková R, Sýkorová J, Prokop Z, Jesenská A, Monincová M, Pavlová M, et al. Modification of activity and specificity of haloalkane dehalogenase from *Sphingomonas paucimobilis* UT26 by engineering of its entrance tunnel. J Biol Chem 2003;278: 52622–8. <http://dx.doi.org/10.1074/jbc.M306762200>.
- [15] Ghisla S, Massey V. Mechanisms of flavoprotein-catalyzed reactions. Eur J Biochem 1989;181:1–17. <http://dx.doi.org/10.1111/j.1432-1033.1989.tb14688.x>.
- [16] Massey V. Introduction: Flavoprotein structure and mechanism. FASEB J 1995;9: 473–5. <http://www.fasebj.org/content/9/7/473.full.pdf+html>.
- [17] Mortl M, Diederichs K, Welte W, Molla G, Motteran L, Andriolo G, et al. Structure–function correlation in glycine oxidase from *Bacillus subtilis*. J Biol Chem 2004;279: 29718–27. <http://dx.doi.org/10.1074/jbc.M401224200>.